2021 IEEE Energy Conversion Congress and Exposition (ECCE) | 978-1-7281-5135-9/21/$31.00 ©2021 IEEE | DOI: 10.1109/ECCE47101.2021.9595370

Three-phase Motor Drive Topology with the Fault-tolerant Capability of Open-circuit on the Multiplexing Bridge

Xiangwen Sun
State Key Laboratory of Advanced Electromagnetic Engineering and Technology
Huazhong University of Science and Technology
Wuhan, China
sunxw@hust.edu.cn

Zicheng Liu
State Key Laboratory of Advanced Electromagnetic Engineering and Technology
Huazhong University of Science and Technology
Wuhan, China
liuzc@hust.edu.cn

Zhekai Li
State Key Laboratory of Advanced Electromagnetic Engineering and Technology
Huazhong University of Science and Technology
Wuhan, China
u201810950@hust.edu.cn

Qianchen Sun
State Key Laboratory of Advanced Electromagnetic Engineering and Technology
Huazhong University of Science and Technology
Wuhan, China
qianchensun@hust.edu.cn

An Li
State Key Laboratory of Advanced Electromagnetic Engineering and Technology
Huazhong University of Science and Technology
Wuhan, China
anli@hust.edu.cn

Dong Jiang
State Key Laboratory of Advanced Electromagnetic Engineering and Technology
Huazhong University of Science and Technology
Wuhan, China
jiangd@hust.edu.cn

***Abstract*—The three-phase series-end winding motor drive (SWMD), which connects the three-phase windings in series with identical polarity, is attracting attention due to excellent drive performance. However, when the fault occurs on the center bridges that are multiplexed, smooth torque output capability cannot be obtained anymore, which narrow the applications of SWMD for high reliability requirement. This paper proposes a SWMD with new connection mode of phase windings. Without extra hardware expense, the proposed topology can tolerant the open-circuit of the multiplexing bridge, which greatly improve the reliability of drive system. Experimental results are presented to verify the fault tolerance of the topology.**

Keywords—motor drive, induction machine, three-phase motor, open-end, bridge multiplexing, fault-tolerant control

I. Introduction

With the development of power electronics and motor drive technology, various motor drive topologies have been proposed to optimize motor performance like speed operation range or reliability [1-7]. Generally, the more bridge arms, the better the driving performance. The full-bridge topology possesses obvious advantages over half-bridge topology in voltage utilization, control freedom and fault-tolerant capability [8-10]. However, doubled switching device numbers represent expensive hardware cost and bulky system volume, which hinders the application of full-bridge type in cost-sensitive areas and limit the power density of drive system.

In order to achieve better driving performance than half-bridge topology and reduce the number of switching devices, the bridge multiplexing method is raised and adopted in more and more researches[11-14]. Take three-phase as an example, the typical delta-type driving topology can be seen as a three bridge-multiplexing solution derived from full-bridge, shown in Fig. 1(b). Compared with half-bridge structure, higher voltage utilization is realized with uncontrolled zero-sequence current loop. Meanwhile, this structure cannot generate steady circular magnetomotive force (MMF) when the open-circuit happens on any bridge [11-12], fragile fault-tolerant capability shows weak competitiveness in high-reliability fields. Recently, a two bridge-multiplexing solution which is called series-winding motor drive (SWMD) is attracting more attention due to high voltage utilization and complete control freedom [13-14], shown in Fig. 1(c). where three phase windings are connected in series, and then four nodes are led out and connected to four inverter legs respectively.

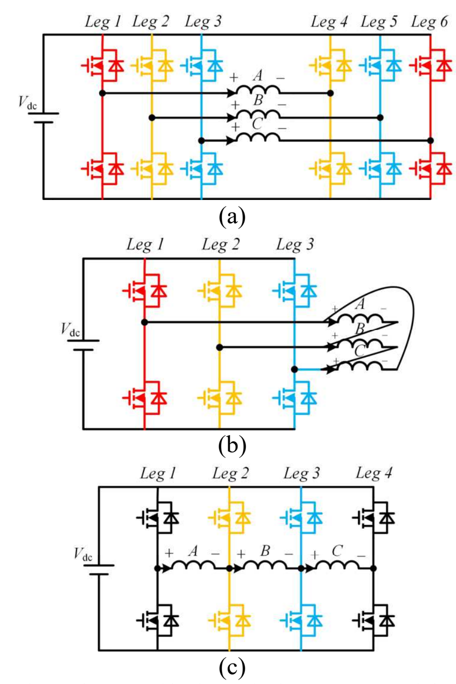

Fig. 1. Scheme diagram of bridge-multiplexing: (a) typical three-phase full-bridge topology. (b) three bridge-multiplexing solution. (c) two bridge-multiplexing solution.

It can be easily found that different bridge multiplexing methods has significant diversity in performance. Compared with half-bridge structure, the delta topology mainly improves the voltage utilization. The SWMD increases the voltage utilization while obtaining zero-sequence controllability. Nevertheless, when the open-circuit fault occurs on the middle multiplexing bridges (draw in yellow or blue), the motor cannot further produce smooth torque if no hardware switching procedure is adopted. Generally, the above two multiplexing methods do not bring obvious reliability improvement.

When only four bridges (or less) are used, the 3+1 bridge topology, which is equivalent to the three-phase half-bridge equipped with another bridge in the neutral point, owes the most comprehensive fault tolerance [15-16]. It can withstand open-circuit failure in any phase winding or any bridge. But the neutral bridge needs to be designed with higher stress margin for faulty condition and it is not fully utilized during normal condition. Hence there is no derating improvement (higher postfault voltage utilization/torque capacity) for 3+1 topology.

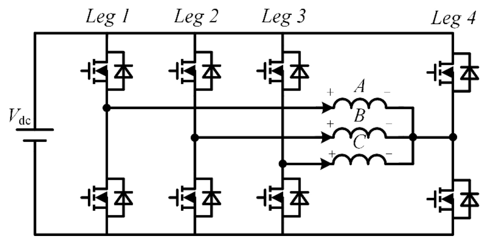

Fig. 2. The topology of 3+1 bridge.

In this paper, a novel two bridge-multiplexing solution for three-phase SWMD is proposed. Compared with existing series-end wingding structure, the new topology can withstand open-circuit failure in multiplexing bridge, which overcomes the original shortcoming of SWMD. Moreover, when the fault occurs on the multiplexing bridge, the derating of torque can be enhanced through analysis.

The organization of this paper is as below: The topology principle in normal condition and corresponding math model are introduced in Section II. Then the several fault types are classified and the fault tolerant theory of the three-phase drive are illustrated in Section III, while the winding loss calculation and comparison are given. The control scheme of the topology is revealed in Section IV. Experimental setup and results in Section V verify the effectiveness of the proposed topology.

II. Principle of Operation in Healthy Conditoin

A. Topology Principle

The proposed two-bridge multiplexing solution with fault-tolerant capability of multiplexing bridge is shown in Fig. 3(a). Compared with original three-phase SWMD, the biggest difference is the connection mode of B-phase winding. In the new solution, the positive end is connected to Leg3 and the negative end is connected to Leg2. Then we can easily obtain the equation:

$$\begin{bmatrix} v_A \\ v_B \\ v_C \end{bmatrix} = \begin{bmatrix} 1 & -1 & 0 & 0 \\ 0 & -1 & 1 & 0 \\ 0 & 0 & 1 & -1 \end{bmatrix} \begin{bmatrix} v_{leg1} \\ v_{leg2} \\ v_{leg3} \\ v_{leg4} \end{bmatrix} \tag{1}$$

Where $v_A \sim v_C$ are the phase winding voltages and $v_{leg1} \sim v_{leg4}$ are output voltages of inverter bridges. It can be found that the numbers of bridges is one more than the winding, the topology can control the zero-sequence component actively. Moreover, when the three-phase winding voltage is determined, there are infinite solutions to meet (1). We choose the solution with balanced bridge outputs [17], shown in Fig. 4. The mathematical relationship can be represented as :

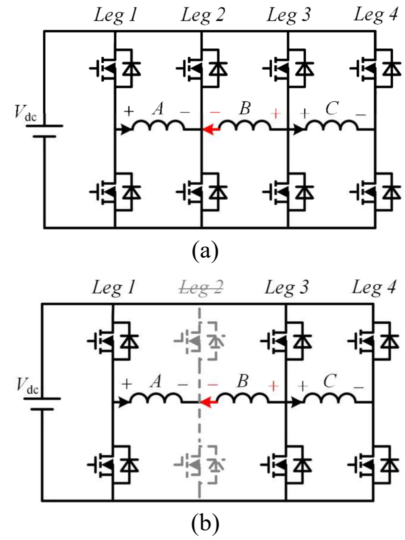

Fig. 3. Proposed three-phase series-end winding drive topology: (a) Normal condition. (b) After the fault occurs on the multiplexing bridge.

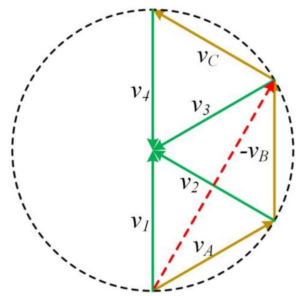

Fig. 4. The voltage relationship between the phase winding and bridge output.

$$\begin{aligned} v_{leg1} &= -v_B \\ v_{leg2} &= v_C \\ v_{leg3} &= -v_A \\ v_{leg4} &= v_B \end{aligned} \tag{2}$$

Through Equation (2), the bridge modulation signal can be gotten with the references of conventional vector control. No extra modulation is needed.

III. Principle of Operation in Fault Conditoin

A. Classified Fault Conditions

The failures of switching devices or windings are mainly divided into open-circuit and short-circuit failures. When short-circuit occurs in many applications, the blown fuse will remove the fault phase, which is similar to open-circuit fault in electrical characteristic.

For traditional three-phase half bridge topology, it has no difference whether the fault occurs on the winding or devices when the anti-parallel diode is not considered. However, the current restriction brought by inverter failure is not completely equivalent to that by winding failure for the proposed topology. The classification of fault conditions should be made to separately discuss the postfault driving characteristics. According to the postfault structure diversity, the seven failure conditions can be divided into two categories.

The first category involves the failures of leg1, leg4 or three-phase windings, which results in the zero current of the single phase, while the other two-phase currents are not restricted. To keep magnetmotive force (MMF) constant, the postfault current distribution should meet the following: (Take the failure of phase A as an example)

$$\begin{aligned} &MMF_H = i_A \cos\theta + i_B \cos(\theta - \frac{2}{3}\pi) + i_C \cos(\theta - \frac{4}{3}\pi) \\ &MMF_{F\text{-}I} = i_{BF} \cos(\theta - \frac{2}{3}\pi) + i_{CF} \cos(\theta - \frac{4}{3}\pi) \\ &MMF_H = MMF_F \end{aligned} \quad (3)$$

Where i_A=$I_m$cos(ωt), i_B=$I_m$cos(ωt-2π/3), i_C=$I_m$cos(ωt-4π/3) are the phase currents in healthy condition. i_{BF}~ i_{CF} are the postfault currents after the open-circuit fault occurs on the Phase A. Then we can get:

$$i_{AF} = i_A - i_A = 0,\ \ i_{BF} = i_B - i_A,\ \ i_{CF} = i_C - i_A \quad (4)$$

The postfault current distribution equals to the healthy three-phase currents with superposition of a common zero-sequence component that opposite to the faulty phase (depicted in Fig. 5). The faults in this category has been researched in many publications [1,5-6,11-12] and will not be discussed in detail here.

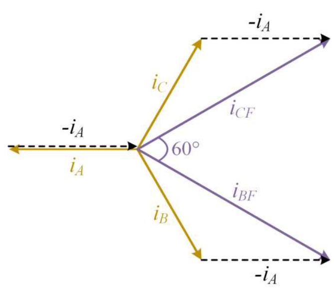

Fig. 5. The phase current distribution before and after the fault occurs in Category I.

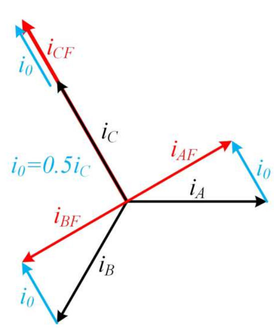

Fig. 5. The phase current distribution before and after the fault occurs in Category II.

The second category represents the failure of Leg2 or Leg3, which means two windings are flowed through the same currents, depicted in Fig. 3(b) (Take the fault of Leg2 as an example). Two windings, phase A and phase B are connected in series and driven by Leg1 and Leg3. The postfault restriction on the current can be represented as:

$$i_{AF} = -i_{BF} \quad (5)$$

It worth noting that the negative sign is caused by the reverse connection of the B-phase winding. If we substitute the restriction without negative sign to (3), no solution can be found, which shows the SWMD with positive connection of B-phase cannot withstand the open-circuit of category II.

For proposed topology, the postfault current distribution satisfying both constant MMF and Equation (5) can be solved:

$$\begin{aligned} &i_{AF} = \frac{\sqrt{3}}{2} I_m \cos(\omega t + \frac{\pi}{6}) \\ &i_{BF} = -\frac{\sqrt{3}}{2} I_m \cos(\omega t + \frac{\pi}{6}) \\ &i_{CF} = \frac{3}{2} I_m \cos(\omega t - \frac{4\pi}{3}) \end{aligned} \quad (6)$$

Corresponding current vector distribution is depicted in Fig. 5. The postfault currents (red) can be seen as the symmetrical three-phase currents (black) are superimposed with zero-sequence component (blue) which do no contribution to MMF. The magnitude of C-phase current is increased by 50% due to the injection of zero-sequence component, while the amplitude of A- and B-phase currents decrease. The asymmetrical current distribution results in the C-phase current reaches the limited rated value first, which can be used to analysis postfault derating influence.

In the faults of category II, the maximum phase current becomes 150% of the healthy value with constant MMF, hence the torque output capability is decreased to 66% of rated value. Compared to conventional faults of category I which can only achieve 57% of rated output [6], the proposed topology owes less capacity reduction with complete fault tolerance.

Besides, the postfault winding losses should be calculated to estimate the system efficiency decrease under the same working condition:

$$\begin{aligned} &J_{\mathrm{H}} = 1^2 + 1^2 + 1^2 = 3 \\ &J_{\mathrm{F\text{-}I}} = (\sqrt{3})^2 + (\sqrt{3})^2 = 6 \\ &J_{\mathrm{F\text{-}II}} = 1.5^2 + (\sqrt{3}/2)^2 + (\sqrt{3}/2)^2 = 3.75 \end{aligned} \quad (7)$$

Where J represent the sum of winding losses and take the phase current in healthy condition as unit 1. It can be easily concluded that the postfault winding losses would rise regardless of any fault. Nevertheless, the losses are doubled in Category I and increased 25% in Category II. Which shows that the system can achieve better operation efficiency in Category II.

IV. CONTROL SCHEME

The control scheme of the system is shown in Fig.6. there are two closed control loops: the outer speed loop, which is set to regulate the speed of motor with providing torque reference using single PI controller, and the inner current loop, which is set to adjust output command to control torque and maintain flux linkage stable using two PI controllers. The calculated dq-axis output voltage should be transformed to stationary coordinate by inverse park transformation. Through the redistribution in (2), we can get the desired bridge output.

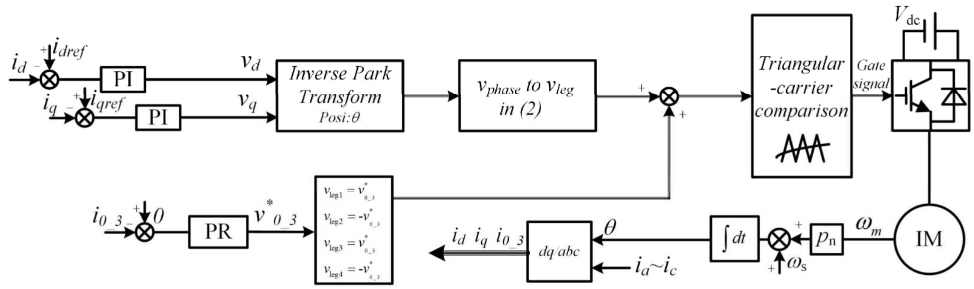

Fig. 6. The control scheme diagram.

The existing of the zero-sequence pathway ensures the proposed topology can acquire satisfying fault-tolerant basis. However, all the zero-sequence components can flow the pathway. Concerning there is obvious zero-sequence components of three times the fundamental frequency in the EMF of actual motors, the specific PR controller is adopted. It is worth distinguishing that the zero-sequence suppression here only focuses on the components of three-times the fundamental frequency 3ωt, resulted from the non-ideal motor EMF. No zero-sequence component at fundamental frequency is influenced by suppression. The zero-sequence control complies with:

$$\begin{aligned} v_{\text{leg1}} &= v^*_{0\_3} \\ v_{\text{leg2}} &= -v^*_{0\_3} \\ v_{\text{leg3}} &= v^*_{0\_3} \\ v_{\text{leg4}} &= -v^*_{0\_3} \end{aligned} \tag{8}$$

We choose the traditional induction motor as the test object, the existing slip frequency should be calculated through current sensors and combine the speed information from encoder to measure rotor flux angle. The motor parameters used in the calculation are obtained from no-load and short circuit test.

V. EXPRIMENTAL RESULTS

TABLE I
PARAMETERS OF INDUCTION MACHINE

Parameter	Value	Parameter	Value
Pole Pairs	1	Rated Power (kW)	2.2
Rated Voltage (V)	220	Rated Current (A)	4.75
Rated Speed (rpm)	2890	Stator Self-Inductance (mH)	269.2
Stator Resistance (Ω)	2.876	Stator Leakage Inductance (mH)	9.5

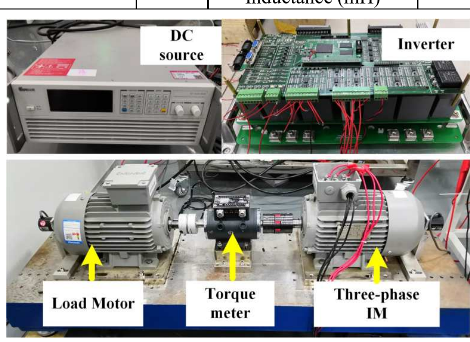

Fig 7. Photograph of the motor drive platform.

To validate the fault-tolerant feasibility of the proposed topology for three-phase open-end induction motor drive (Corresponding parameters are shown in TABLE I), experiments were conducted on a three-phase motor platform, shown in Fig. 7, with a conventional three-phase IM fed by a commercial converter acting as the load. A general inverter is employed to feed the tested IM, which has six half bridge inverter legs composed of two IGBT modules (FS100R12KT4G from Infineon, V_{cemax}=1200V, I_N=100A). The proposed control method has been implemented using a DSP TMS320F28377D controller board from Texas Instrument. The switching frequency is 10kHz and the leg deadtime is set to 1μs. It should be noted that the fault diagnosis is not necessary for the topology. The open-circuit fault is realized by opening the breaker.

A. Fault-Tolerant Test

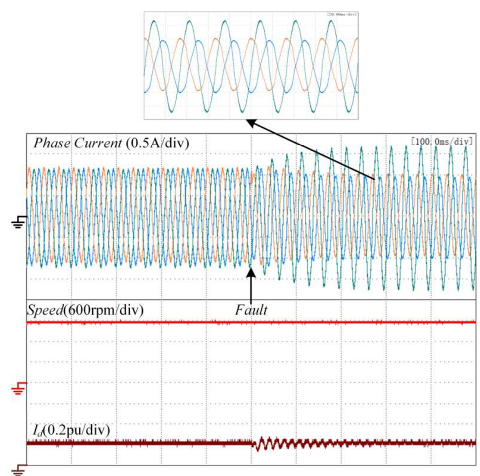

Fig. 8. The open-circuit test results.

The fault transient test is carried out under the speed of 1800rpm in Fig. 8. The fault is with Leg2 to be open-circuited by opening the breaker. The three phase currents are given to show current distribution information, and the *d*-axis current from positive-sequence transformation can represent the motor flux information (torque value and ripple) Before the fault occurs, the three-phase currents are symmetrical. The current amplitude of each phase is about 1.15A.

Then the gate drive signal of Leg2 is locked by fault, the results show that the motor can effectively withstand the assault caused by open-circuit failure of multiplexing bridge. Particularly, the total fault-tolerant procedure is executed without the assistance of the extra hardware or real-time working fault diagnosis, which shows the satisfying fault tolerance to deal with unexpected failures. It can be found that a flux ripple emerges when the fault just happened. It was caused by fault-induced negative-sequence component and suppressed in less than 300ms.

In postfault steady state, new three-phase current distribution can be detected from Fig. 8. C-phase current is with the magnitude of 1.63A. A- and B-phase current is with the magnitude of 1A. The load is constant before and after the fault. Hence the C-phase current is increased by 42% (1.42 times of healthy value), and the A- and B-phase current are decreased by 13% (0.87 times of healthy value). The postfault current magnitude variation is almost identical to the theory calculation. The existing error is mainly resulted by the nonideal factors like current harmonic.

The dynamic response test is executed in Fig. 9. The reference speed is stepped from 1800rpm to -1800rpm. The faulty three-phase system finished the reversal rotation in 1.1s. From the perspective of faulty system, the dynamic response performance in transient condition is still satisfying, without the need to adjust PI parameters.

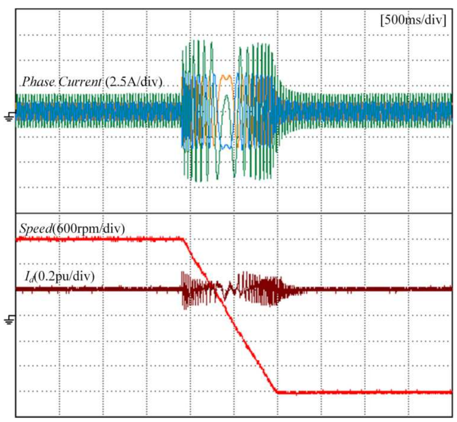

Fig. 9. The dynamic response test of reversal rotation.

VI. Conclusion

Exsisting three-phase open-end wingding topologies with multiplexing bridge have big defects in reliability, especially when the open-circuit fault occurs on the multiplexing bridge, the system cannot further continue generate smooth torque. This paper proposes a novel three-phase series-end wingding topology, in which the B-phase winding is connected with reverse connection. All possible faults are discussed and classified into two categories. Through the analytical results based on postfault structures, a simplified and practical control method is proposed for the topology, which can help the system withstand the fault of any phase or any bridge without special real-time fault diagnosis. Relative experiments have been conducted to prove the feasibility of method.

Acknowledgment

This work is sponsored by National Natural Science Foundation of China under Project No.51707007, No.52077088 and the Fundamental Research Funds for the Central Universities 2021yjsCXCY002.

References

[1] M. Tousizadeh, H. S. Che, J. Selvaraj, N. A. Rahim and B. Ooi, "Performance Comparison of Fault-Tolerant Three-Phase Induction Motor Drives Considering Current and Voltage Limits," in *IEEE Transactions on Industrial Electronics*, vol. 66, no. 4, pp. 2639-2648, April 2019.

[2] X. Sun, Z. Liu, D. Jiang and W. Kong, "Multiphase Open-End Winding Induction Machine Drive With the Floating Capacitor," in *IEEE Transactions on Industry Applications*, vol. 56, no. 5, pp. 5013-5022, Sept.-Oct. 2020.

[3] M. Tousizadeh, H. S. Che, J. Selvaraj, N. A. Rahim and B. Ooi, "Fault-Tolerant Field-Oriented Control of Three-Phase Induction Motor Based on Unified Feedforward Method," in IEEE Transactions on Power Electronics, vol. 34, no. 8, pp. 7172-7183, Aug. 2019.

[4] Z. Liu, Z. Zheng, Q. Wang and Y. Li, "Enhanced rotor field-oriented control of multiphase induction machines based on symmetrical components theory," in *IET Power Electronics*, vol. 12, no. 4, pp. 656-666, 10 4 2019.

[5] H. T. Eickhoff, R. Seebacher, A. Muetze and E. G. Strangas, "Post-Fault Operation Strategy for Single Switch Open-Circuit Faults in Electric Drives," in IEEE Transactions on Industry Applications, vol. 54, no. 3, pp. 2381-2391, May-June 2018.

[6] Z. Liu, Z. Zheng, L. Xu, K. Wang and Y. Li, "Current Balance Control for Symmetrical Multiphase Inverters," in *IEEE Transactions on Power Electronics*, vol. 31, no. 6, pp. 4005-4012, June 2016.

[7] C. Zhu, Z. Zeng and R. Zhao, "Comprehensive Analysis and Reduction of Torque Ripples in Three-Phase Four-Switch Inverter-Fed PMSM Drives Using Space Vector Pulse-Width Modulation," in IEEE Transactions on Power Electronics, vol. 32, no. 7, pp. 5411-5424, July 2017.

[8] W. Hu, C. Ruan, H. Nian and D. Sun, "Simplified Modulation Scheme for Open-End Winding PMSM System With Common DC Bus Under Open-Phase Fault Based on Circulating Current Suppression," in IEEE Transactions on Power Electronics, vol. 35, no. 1, pp. 10-14, Jan. 2020.

[9] Y. Zuo, X. Zhu, X. Si and C. H. T. Lee, "Fault-Tolerant Control for Multiple Open-Leg Faults in Open-End Winding Permanent Magnet Synchronous Motor System Based on Winding Reconnection," in *IEEE Transactions on Power Electronics*, vol. 36, no. 5, pp. 6068-6078, May 2021.

[10] X. Zhang and C. Xu, "Second-Time Fault-Tolerant Topology and Control Strategy for the Open-Winding PMSM System Based on Shared Bridge Arm," in *IEEE Transactions on Power Electronics*, vol. 35, no. 11, pp. 12181-12193, Nov. 2020.

[11] A. Sayed-Ahmed, B. Mirafzal and N. A. O. Demerdash, "Fault-Tolerant Technique for Δ-Connected AC-Motor Drives," in *IEEE Transactions on Energy Conversion*, vol. 26, no. 2, pp. 646-653, June 2011.

[12] A. Sayed-Ahmed and N. A. O. Demerdash, "Fault-Tolerant Operation of Delta-Connected Scalar- and Vector-Controlled AC Motor Drives," in *IEEE Transactions on Power Electronics*, vol. 27, no. 6, pp. 3041-3049, June 2012.

[13] A. Li, D. Jiang, W. Kong and R. Qu, "Four-Leg Converter for Reluctance Machine With DC-Biased Sinusoidal Winding Current," in *IEEE Transactions on Power Electronics*, vol. 34, no. 5, pp. 4569-4580, May 2019.

[14] A. Li, D. Jiang, Z. Liu and X. Sun, "Generalized PWM Method for Series-End Winding Motor Drive," in *IEEE Transactions on Power Electronics*, vol. 36, no. 4, pp. 4452-4462, April 2021.

[15] A. Gaeta, G. Scelba and A. Consoli, "Modeling and Control of Three-Phase PMSMs Under Open-Phase Fault," in *IEEE Transactions on Industry Applications*, vol. 49, no. 1, pp. 74-83, Jan.-Feb. 2013.

[16] H. T. Eickhoff, R. Seebacher, A. Muetze and E. G. Strangas, "Post-Fault Operation Strategy for Single Switch Open-Circuit Faults in Electric Drives," in *IEEE Transactions on Industry Applications*, vol. 54, no. 3, pp. 2381-2391, May-June 2018.

[17] A. Li, D. Jiang, X. Sun and Z. Liu, "Method of Expanding Operating Range for Three-phase Series-end Winding Motor Drive," 2020 *IEEE Energy Conversion Congress and Exposition (ECCE)*, Detroit, MI, USA, 2020, pp. 2020-2025.